Steel and Composite Structures, *Vol. 25, No. 5 (2017) 593-601*
DOI: https://doi.org/10.12989/scs.2017.25.5.593

Numerical investigation of SHS steel beam-columns strengthened using CFRP composite

Amir Hamzeh Keykha*

Department of Civil Engineering, Zahedan Branch, Islamic Azad University, Zahedan, Iran

(*Received August 25, 2016, Revised August 19, 2017, Accepted September 02, 2017*)

Abstract. Carbon Fiber Reinforced Polymer (CFRP) is one of the materials used to strengthen steel structures. Most studies on strengthening steel structures have been done on steel beams and steel columns. No independent study, to the researcher's knowledge, has studied the effect of CFRP strengthening on steel beam-columns, and it seems that there is a lack of understanding on behavior of CFRP strengthening on steel beam-columns. However, this study explored the use of adhesively bonded CFRP flexible sheets on retrofitting square hollow section (SHS) steel beam-columns, using numerical investigations. Finite Element Method (FEM) was employed for modeling. To determine the ultimate load of SHS steel beam-columns, ten specimens, eight of which were strengthened with the different coverage length and with one and two CFRP layers, with two types of section (Type A and B) were analyzed. ANSYS was used to analyze the SHS steel beam-columns. The results showed that the CFRP composite had no similar effect on the slender and stocky SHS steel beam-columns. The results also showed that the coverage length, the number of layers, and the location of CFRP composites were effective in increasing the ultimate load of the SHS steel beam-columns.

Keywords: steel beam-columns; CFRP; strengthening; ultimate load; FE-Method

1. Introduction

Nowadays, due to the increasing cost of rebuilding, retrofitting and strengthening existing structures seem necessary. Although the cost of rebuilding is not an important issue, the cost of maintenance antiquities is of great important. Strengthening and retrofitting structures are different. One way that has been welcomed by researchers is the use of CFRP composites. The use of CFRP composites is a perfect solution in order to overcome the existing shortcomings and strengthen certain infrastructures such as bridges (ACI 440, 2002). Compared to other reinforcement materials, CFRP composite materials is preferred to strengthen steel structures due to the fact that it has higher elastic modulus and ability to be applied in any form of structure. Over the past decades, some studies have been done on strengthening and retrofitting steel columns (Teng and Hu 2007, Bambach *et al.* 2009, Haedir and Zhao 2011, Fanggi and Ozbakkaloglu 2015, Ozbakkaloglu and Xie 2015, Park and Yoo 2013, Kim and Harries 2011, Keykha *et al*. 2015, 2016a, 2016b, 2017b). Other studies have been done on flexural strengthening (Idris and Ozbakkaloglu 2014, 2015, Deng *et al.* 2004, Youssef 2006), shear (Islam and Young 2013), tensile (Al-Zubaidy *et al.* 2013), and torsional of steel beams Abdollahi Chakand *et al*. 2013, Keykha 2017c).

In another investigation, Keykha (2017d) presented a numerical study to investigate the behavior of SHS steel frames. The SHS steel frames were strengthened using CFRP composite on bottom and/or all four corner sides. The results showed that the coverage length and the number of layers of CFRP composite have a significant effect on increasing the ultimate load of the SHS steel frames. Also, the results showed that the location of CFRP composite had no similar effect on increasing the ultimate load and the amount of mid span deflection of the SHS steel frames. Its results showed that, CFRP strengthening significantly increased the ductility capacity for all the SHS steel frames.

The maximum percent of increasing in the ductility capacity was about 826%. Investigations of Keykha in this study showed that in the SHS steel frames of thin walled under contracted loads, duo to the buckling failure is occurred at the top flange, the CFRP sheet is not very effective in the ultimate load capacity while the CFRP sheet is located at the bottom face of the SHS steel frames.

Sundarraja and Prabhu (2013) strengthened the hollow steel beams, which were filled with concrete, using CFRP composites and then they tested. The results showed that the strengthened beams by full wrapping exhibited more enhancements in stiffness and moment carrying capacity. They also presented an economical method for strengthening of the hollow steel beams that were filled with concrete.

In another investigation, Al Zand *et al.* (2015) strengthened the square CFST (concrete-filled steel tube) beams. The results showed that, for all strengthened CFST models using one layer of CFRP sheet, CFRP had no significant enhancement in the ultimate load values when wrapped along 50, 75 and 100% of the length of samples.

Keykha *et al*. (2016a) strengthened the slender square hollow section steel columns with different boundary conditions using CFRP. They offered a theoretical method

*Corresponding author, Ph.D.,
E-mail: ah.keykha@iauzah.ac.ir

ISSN: 1229-9367 (Print), 1598-6233 (Online)

to analyze these columns. The results showed that the CFRP composite did not have the same effect on columns with different conditions.

Idris and Ozbakkaloglu (2016) investigated the seismic behavior of square FRP–concrete–steel columns under combined axial compression and reversed-cyclic lateral loading, using an experimental study. In this study, square double-skin tubular columns (DSTCs) exhibited very ductile behavior under combined axial compression and reversed-cyclic lateral loading. The important influence of the axial load level on the column behavior was evident, with an increase in the load level leading to a significant decrease in the lateral deformation capacity of DSTCs. In the DSTC with a larger inner steel tube, the lateral displacement capacity was lower than the DSTC with a smaller inner steel tube. The results also indicate that, the axial load level, inner steel tube size, and presence of a concrete-filling inside inner steel tube have effect on the plastic hinge lengths of the DSTCs. The results also indicate that, the dimension of inner steel tube has effect on the plastic hinge length through its influence on buckling behavior of the tube. The results of this study showed that, provision of a concrete-filling inside inner steel tube can be significantly increased the progression and length of the plastic hinge region. In another study, Ozbakkaloglu and Idris (2014) investigated the seismic behavior of FRP concrete–steel DSTCs, using an experimental study. They tested DSTCs that were made of high-strength concrete subjected to constant axial compression and reversed-cyclic lateral loading. The results indicated that, the DSTCs are capable of developing very high inelastic deformation capacities subjected to simulated seismic loading. The results also indicated that, the presence of a concrete filling inside the inner steel tube has significantly and positively effect on the seismic behavior of DSTCs. In this study, the results indicate that, the FRP-tube material has effects on the lateral displacement capacity of DSTCs, with the specimens confined by FRP tubes manufactured using fibers with higher ultimate tensile strains developing slightly higher displacement capacities.

Recently, by using CFRP composite, Keykha (2017a) strengthened the SHS steel members having initial deficiencies under combined axial compression and lateral loading. In analyzed deficient specimens, the deficiencies had different lengths and orientation. The results indicated that the initial deficiencies in the SHS steel members decrease the ultimate load carrying capacity of these members. When the deficient was considered in the direction of the width of steel members, the deficient had high impact in decreasing the ultimate load capacity of the steel members. Therefore, in the steel members with a transverse deficient, CFRP had a considerable impact in the ultimate load capacity of these specimens.

From the past studies, it can be observed that there were investigations done with the use of CFRP composite as a strengthening material for SHS steel members. It seems that there is a lack of understanding on the behavior of slender and stocky steel beam-columns strengthened using CFRP composite. Therefore, this article aimed to develop the knowledge in this area. For this purpose, this study explored the use of adhesively bonded CFRP flexible sheets on retrofitting SHS steel beam-columns, using numerical investigations. In order to carefully examine, both slender SHS steel beam-columns (Type B) and stocky (Type A) were analyzed. The coverage length, the number of layers, and the location of CFRP composite were implemented to examine the ultimate load of the SHS steel beam-columns.

2. Material used

The dimensions, the section types, and properties of the consumed steel in this study are given in Table 1. The yield strength mean value found by coupon tests is 280 N/mm^2 and the ultimate tensile strength mean value is 375 N/mm^2. The consumed CFRP in the present research is SikaWrap-230C. Properties of CFRP composite are shown in Table 2. Adhesive used in this study is suggested by the supplier of CFRP product. The adhesive is commonly used for the SikaWrap-230C, called Sikadur-330 (Table 3).

3. Finite element modeling

3.1 Model description

Non-linear finite element models were prepared using ANSYS to investigate the structural behavior of the SHS steel beam-columns strengthened by CFRP sheets in length.

All models were prepared as fixed-pinned supported beam-columns with two pint loads, at which one of the load was axial compression load (P) and another load was lateral load (Q). The axial compression load was applied at the top of beam-columns, and the lateral load was applied in the mid-span of the SHS steel beam-columns.

Table 1 Sizes and properties of SHS steel

Type section	Dimensions (h × b × t) (mm)	Length L (mm)	Modulus of elasticity (N/mm^2)	Stress (N/mm^2) Yielding (F_y)	Ultimate (F_u)
A	90 × 90 × 2.5	3000	200000	280	375
B	40 × 40 × 2.0	3000	200000	280	375

Table 2 Properties of CFRP material

CFRP Sheet: SikaWrap-230C				
Fabric design thickness (mm)	Modulus of elasticity (N/mm^2)	Ultimate tensile strength (N/mm^2)	Ultimate tensile elongation (%)	Thickness (Impregnated with Sikadur-330) (mm)
0.131	238000	4300	1.8	1

Table 3 Properties of adhesive

Adhesive: Sikadur-330			
Tensile strength (N/mm^2)	Modulus of elasticity (N/mm^2)		Elongation at break (%)
	Tensile	Flexural	
30	4500	3800	0.9

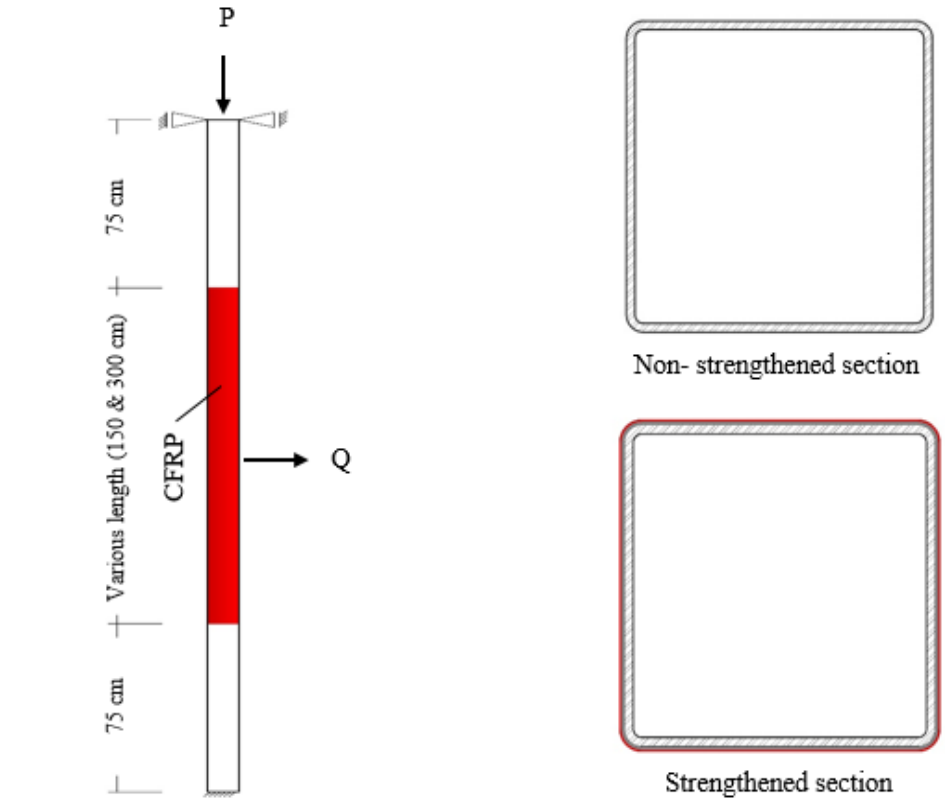

(a) SHS steel beam-columns-side view (b) Cross section

Fig. 1 Boundary conditions of a SHS steel beam-column strengthened using CFRP

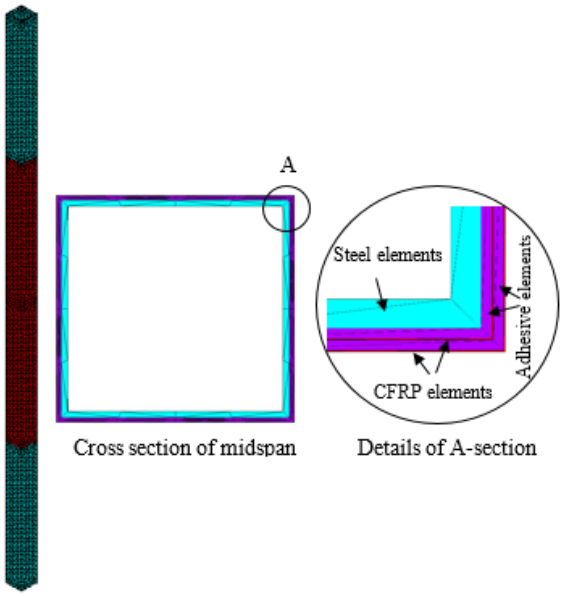

Fig. 2 Finite element modeling (specimen AC2-50)

Fig. 1 shows the boundary conditions of the SHS steel beam-columns and the strengthening scenario adopted in this study.

Fig. 2, for instance, shows three dimensional (3D) finite element model of the prepared specimens using ANSYS (specimen AC2-50). The axial compression load and the lateral load were simultaneously applied to the beam-columns. These loads gradually increased until the strengthened SHS steel beam-columns achieved their ultimate load capacity.

Table 4 Ultimate load of specimen BC0 in analyzing numerical and experimental (Keykha *et al*. 2015)

Experimental result (kN)	Simulation results in ANSYS (kN)				
	Size mesh	10 node 187	20 node 186	Tet 4 node 285	Brick 8 node 185
31.80	10	31.02	32.09	24.50	37.01
	15	31.31	32.22	25.49	40.51
	20	31.66	32.41	26.69	41.59
	25	31.85	32.63	26.93	43.46
	30	32.12	33.60	26.97	45.79

Table 5 Ultimate loads of specimen BC0 and BC2-50 in analyzing numerical and experimental

Specimen label	No. of layers CFRP	Experimental ultimate load (kN)	Numerical ultimate load (kN)	Error (%)
BC0	0	31.80	31.85	0.16
BC2-50	2	37.80	37.60	0.52

3.2 Element description

The application of accurate scientific software in modeling and simulation of scientific problems has been increased recently. One of the most powerful analytical tools which is widely used in mechanical and civil engineering is ANSYS software. The solution of problems in the ANSYS software is based on the finite element method which is a numerical analyzing method. In this research, materials were considered in the form of 3D models. SOLID elements is used in these models (Keykha *et al*. 2016a).

3.3 Meshing convergence study

In ANSYS software, several SOLID elements are available such as 10 node 187, 20 node 186, Tet 4 node 285, Brick 8 node 185, and so on. To determine an appropriate mesh size, the specimen BC0, which was tested by Keykha *et al*. (2015), is analyzed with these four elements and different mesh size. For analyzing of the specimens, non-linear static analysis was carried out to achieve the failures. In this case, the load was incrementally applied until the plastic strain in an element reached to its ultimate strain (element is killed). Linear and non-linear properties of materials were defined. The CFRP sheets material properties were defined as linear and orthotropic because CFRP materials have linear properties and they were unidirectional. Also, the adhesive was defined as linear materials because the adhesive has linear properties (Keykha *et al.* 2016a). The SHS steel beam-columns was defined as the materials having non-linear properties. Results showed that, the solid element of 187 and 185 were appropriate (see Table 4). With an increase in the number of element nodes and with a decrease in the mesh size, the calculation time increases. Therefore, in this study to reduce the calculation time, the solid element of 187 (the number of element nodes of 187 less than the number of element nodes of 185) with the mesh size of 25 was selected (Table 4).

3.4 Validity of software results

It is necessary to validate the calculation of software. In this study, the software results were validated and calibrated by the experimental results of Keykha *et al.* (2015). For the analysis of the specimens, as mentioned in the previous section, the solid element of 187 with the mesh size of 25 was selected (Keykha *et al*. 2016a). Both numerical and result experimental (Keykha *et al.* 2015) for specimen BC2-50 and the specimen BC0 are shown in Table 5.

Figs. 3(a) and 3(b) show a simulated specimen using ANSYS software and an experimental tested specimen. The compression load-displacement curve of the specimen BC2-50, obtained from both experimental and numerical results, is also displayed in Fig 4. As shown in Fig. 4, good accuracy is seen between the experimental and the numerical results.

3.5 Description of specimens

The beam-columns are included two control specimens and eight specimens strengthened with one and two layers of CFRP applied on all four sides of the beam-columns. In each type (Type A and Type B) of beam-columns, to determine the increase rate of the ultimate load in strengthened steel beam-columns, one specimen without strengthening, as control specimen, was analyzed. To easily identify the specimen, the beam-columns were designated by the names such as AC0, AC1-50, AC2-50, AC1-100, AC2-100, BC0, BC1-50, BC2-50, BC1-100 and BC2-100. For example, the specimens AC2-100 and BC2-100 indicate that they were strengthened by two layers of CFRP fully wrapped around the beam-columns Type A and B, respectively. The specimen AC2-50 indicates that it is a Type A beam-column strengthened by two layers and the CFRP coverage 50% wrapped around the beam-column. The specimen BC1-50 also specifies that it is a Type B beam-column strengthened by one layer and the CFRP coverage 50% wrapped around the beam-column. Similarly, the specimen BC2-50 specifies is a Type B beam-column strengthened by two layers and the CFRP coverage 50% wrapped around the beam-column. The control beam-columns of Type A and B are designated as AC0 and BC0, respectively.

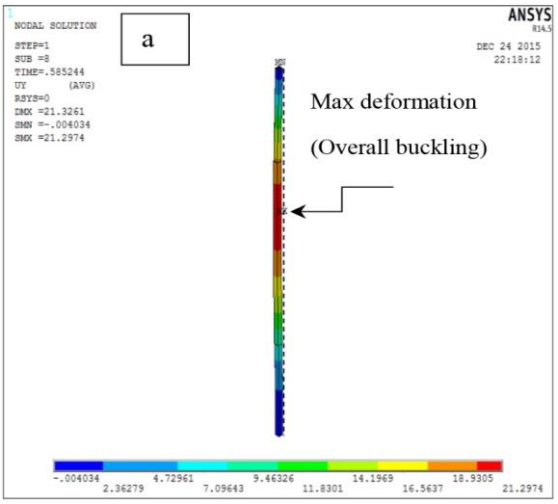

(a) The specimen BC2-50 in numerical simulation

(b) The specimen BC2-50 in experimental test (Keykha *et al*. 2015)

Fig. 3 Failure mode of specimen BC2-50

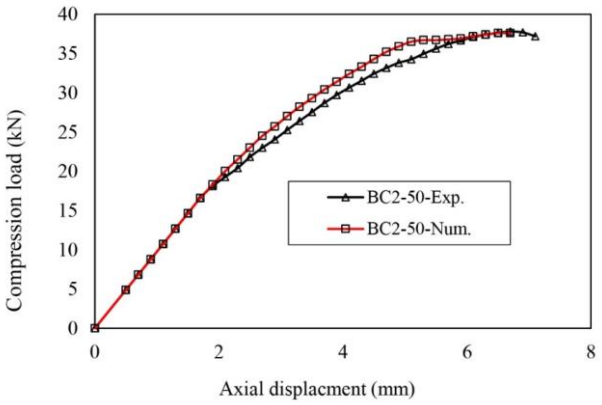

Fig. 4 Compression load-displacement curve of specimen BC2-50, numerical and experimental (Keykha *et al*. 2015)

4. Results and discussion

4.1 The ultimate load results

Tables 6 and 7 show the numerical analysis results of the specimens in Type A and B without strengthening or with one or two layers of CFRP sheet strengthened. The coverage length of CFRP varies based on the length of beam-columns. The center position of CFRP sheet is in the center of beam-column. The results showed that in the Type A beam-columns (stocky beam-columns) when the CFRP coverage percentage is less than 100%, if the lateral load is equal to zero, CFRP is not effective in the ultimate compression load of beam-columns. With an increase in the lateral load and a decrease in the axial compression load, the rate of increase of the ultimate load in beam-columns increases. The percentage of increase of the ultimate load in the lateral load is more than the axial compression load. For Type A beam-columns, when the CFRP coverage is full, the CFRP sheet is effective in the ultimate compression load, even if the lateral load is equal to zero. The maximum percentage of increase in the ultimate load happened for the specimen AC2-100 (124.15%) in the lateral load. This specimen (specimen AC2-100) was strengthened with two layers and the coverage length 100% of CFRP sheet.

In contrast to the Type A beam-columns, in the Type B beam-columns (slender beam-columns) when the CFRP coverage percentage is less than 100%, the CFRP sheet is effective in the ultimate compression load of beam-columns. In other words, the ultimate compression load of beam-columns increases when the lateral load is equal to zero or non-zero. Similar to the Type A beam-columns, in the Type B beam-columns, with an increase in the lateral load and a decrease in the axial compression load, the rate of increase of the ultimate load in the beam-columns increases. The maximum percentage of increase in the ultimate load happened for the specimen BC2-100 (80.10%) in the lateral load.

4.2 Failure modes

All specimens were subjected to two point loads until failure. One of the loads was applied on top (the axial compression load of P) and another load was applied in mid-span (the lateral load of Q) of the beam-columns. When the lateral loads were equal to zero, in the Type A beam-columns, a local buckling was observed on the top under the axial compression loads (Fig. 5(a)). With an increase in the lateral load, the failure modes of the beam-columns changed to local buckling and overall buckling, in near mid-span (Fig. 5(b)).

In the Type B beam-columns, the failure modes of all specimens are the same, and are the overall buckling. For example, two failure modes from these specimens are shown in Figs. 5(c) and 5(d).

Table 6 Analysis results for specimens of Type A

Specimen label	The simultaneous loads applied to beam-columns (P and Q) and % of increase in loads							
AC0	P (kN)	213.18	178.70	144.29	107.28	67.10	32.35	0.00
	Q (kN)	0.00	1.58	3.18	4.57	5.57	6.17	6.75
AC1-50	P (kN)	214.12	183.73	153.20	116.30	75.59	36.95	0.00
	Q (kN)	0.00	1.62	3.55	5.15	6.59	7.53	8.34
	% of increase in P	0.44	2.81	6.18	8.41	12.65	14.22	0.00
	% of increase in Q	0.00	2.53	5.35	12.69	18.31	22.04	23.56
AC2-50	P (kN)	214.12	186.77	156.38	125.85	80.09	39.34	0.00
	Q (kN)	0.00	1.66	3.47	5.60	8.93	9.59	11.35
	% of increase in P	0.44	4.52	8.38	17.31	19.36	21.61	0.00
	% of increase in Q	0.00	5.06	9.12	22.54	60.32	55.43	68.15
AC1-100	P (kN)	240.24	202.62	169.65	128.85	83.50	41.29	0.00
	Q (kN)	0.00	1.78	3.76	5.69	7.67	8.36	9.25
	% of increase in P	12.69	13.39	17.58	20.11	24.44	27.64	0.00
	% of increase in Q	0.00	12.66	18.24	24.51	37.70	35.49	37.04
AC2-100	P (kN)	289.44	245.62	206.24	170.76	110.96	62.20	0.00
	Q (kN)	0.00	2.14	4.57	7.61	12.38	13.83	11.00
	% of increase in P	35.77	37.45	42.93	59.17	65.37	92.27	0.00
	% of increase in Q	0.00	35.44	43.71	66.52	122.26	124.15	62.96

Table 7 Analysis results for specimens of Type B

Specimen label	The simultaneous loads applied to beam-columns (P and Q) and % of increase in loads							
BC0	P (kN)	31.85	25.19	21.02	16.06	9.73	5.82	0.00
	Q (kN)	0.00	0.31	0.60	0.95	1.50	1.81	3.82
BC1-50	P (kN)	35.06	27.92	23.44	18.21	11.11	6.80	0.00
	Q (kN)	0.00	0.35	0.68	1.09	1.73	2.10	4.63
	% of increase in P	10.08	10.84	11.51	13.39	14.18	16.84	0.00
	% of increase in Q	0.00	12.90	13.33	14.74	15.33	16.02	21.20
BC2-50	P (kN)	37.60	29.85	25.00	19.56	12.21	7.83	0.00
	Q (kN)	0.00	0.37	0.73	1.17	1.87	2.43	6.40
	% of increase in P	18.05	18.50	18.93	21.79	25.49	34.54	0.00
	% of increase in Q	0.00	19.35	21.67	23.16	24.67	34.25	67.54
BC1-100	P (kN)	36.74	29.32	24.65	19.29	12.11	7.62	0.00
	Q (kN)	0.00	0.37	0.72	1.15	1.85	2.36	5.47
	% of increase in P	15.35	16.40	17.27	20.11	24.46	30.93	0.00
	% of increase in Q	0.00	19.35	20.00	21.05	23.33	30.39	43.19
BC2-100	P (kN)	40.89	32.71	27.56	21.93	14.10	9.23	0.00
	Q (kN)	0.00	0.41	0.81	1.32	2.17	2.87	6.88
	% of increase in P	28.38	29.85	31.11	36.55	44.91	58.59	0.00
	% of increase in Q	0.00	32.26	35.00	38.95	44.67	58.56	80.10

4.3 Interaction curves of axial compression -lateral load

The test results such as the ultimate load carrying capacity and the rate of increased ultimate load of the SHS steel beam-columns with respect to the reference beam-columns were summarized in Tables 6 and 7. The results of the ultimate load carrying capacity for the Type A specimens and the Type B specimens are also presented in Figs. 6(a) and 6(b), respectively. In the specimens of Type A, when that the CFRP coverage percent is less than 100%, and the lateral load is equal to zero, the ultimate load carrying capacity of these specimens are not increased with an increase in the number of CFRP layers. In other words, the CFRP composite is not effective in the ultimate compression load.

The reason of no increase in the ultimate compression load in these specimens is that the failure modes of the specimens happened in location out of from the strengthened area (see Fig. 5(a)). With an increase in the lateral load and a decrease in the axial compression load, the failure modes of the specimens happened in location of the strengthened area, and as a result the ultimate load rate of the Type A beam-columns increases. The rate of increase percent in the ultimate lateral load is more than the rate of increase percent in the ultimate compression load. For the Type A beam-columns when the CFRP coverage is full, CFRP is more effective in the ultimate compression load, even if the lateral load is equal to zero. The maximum percentage of the increase in the ultimate load of the Type A beam-columns happened for the specimen AC2-100 (124.15%) in the lateral load, when that the axial

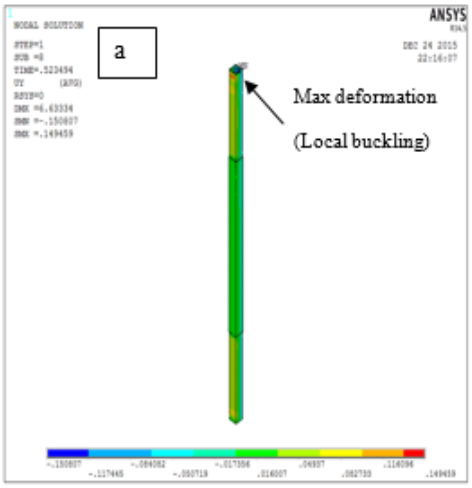

(a) The specimen AC2-50 (in $P \neq 0$ and $Q = 0$)

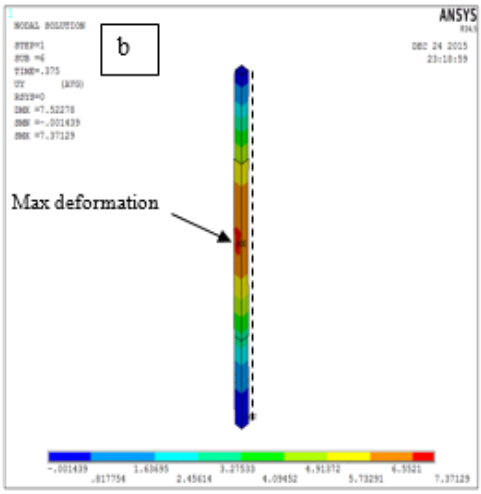

(b) The specimen AC2-50 (in $P \neq 0$ and $Q \neq 0$)

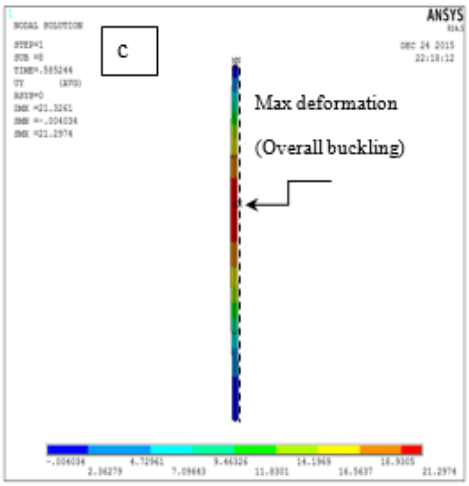

(c) The specimen BC2-50 (in $P \neq 0$ and $Q = 0$)

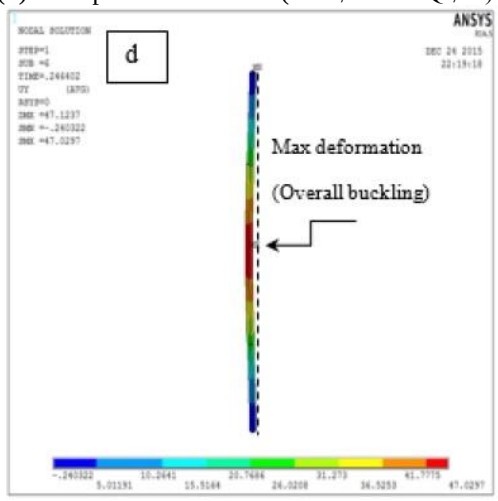

(d) The specimen BC2-50 (in $P \neq 0$ and $Q \neq 0$)

Fig. 5 Failure mode of beam-columns

compression load and the lateral load were 62.20 and 13.83 kN, respectively (Table 6 and Fig. 6(a)).

Fig. 6(b) and Table 7 show that in the Type B beam-columns when the composite coverage percentage is less than 100%, the CFRP sheet is effective in the ultimate compression load. In other words, the ultimate compression load of the Type B beam-columns increases in both cases the lateral load of equal to zero and non-zero. In the Type B beam-columns, similar to Type A beam-columns, with an increase in the lateral load and a decrease in the axial compression load, the rate of increase of the ultimate load increases. The maximum percentage of the load increase in these beam-columns happened for the specimen BC2-100 (80.10%) in the lateral load, when that the axial compression load was equal to zero. In other words, the maximum percentage of the load increase in these beam-columns while happened that the beam-column changed to beam.

5. Conclusions

In this study, the CFRP layers with different in lengths were wrapped around the stocky (the Type A beam-columns) and the slender (the Type B beam-columns) SHS steel beam-columns. The failure modes, the ultimate load carrying capacity, the percentage of the ultimate load increase, and the CFRP wrapping position on the SHS steel beam-columns were discussed. Based on ten analyzed specimens, eight of which were strengthened with the different coverage length and with one and two CFRP layers, the following conclusions can be drawn:

- In stocky beam-columns, when the composite coverage percentage is less than 100%, if the lateral load is equal to zero, CFRP is not effective in the ultimate compression load. The reason of no increase in the ultimate compression load in these beam-columns is that the failure modes of the specimens happened in location out of from the strengthened area (see Fig. 5(a)).

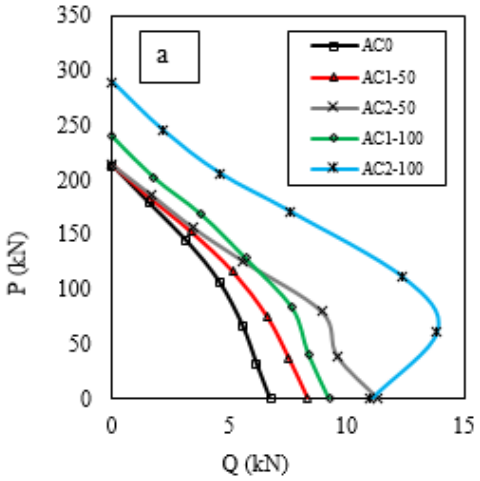

(a) The Type A beam-columns

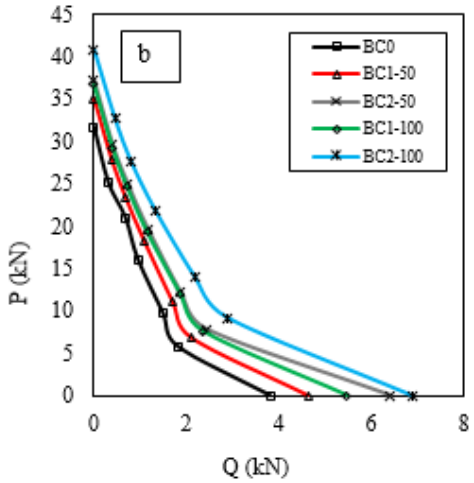

(b) The Type B beam-column

Fig. 6 Interaction curves of the axial compression - lateral load

- With an increase in the lateral load and a decrease in the axial compression load, the rate of the ultimate load increase of the Type A beam-columns increases. The increase percent in the ultimate lateral load is more than the ultimate compression load. In all specimens, the maximum percentage of increase the ultimate load happened for the specimen AC2-100 (124.15%), in the lateral load, when that the axial compression load and the lateral load were 62.20 and 13.83 kN, respectively (see Table 6).
- For Type A beam-columns, when the CFRP coverage is full, CFRP is more effective in the axial compression load. Also, when the lateral load is equal to zero, the amount of increase in the axial compression load rate is 12.69 and 35.77 kN, for the specimens of strengthened with one and two CFRP layers, and full wrapped, respectively.
- In Type B beam-columns, when the composite coverage percentage is less than 100%, the CFRP sheet is effective in the ultimate compression load. In other words, the ultimate compression load of beam-columns increased in both cases the lateral load of equal to zero and non-zero. In these beam-columns, similar to Type A beam-columns, with an increase in the lateral load and a decrease in the axial compression load, the rate of increase of the ultimate load increased. The maximum percentage of increase in the ultimate load happened for the specimen BC2-100 (80.10%), in the lateral load.
- In the beam-column when the lateral load is equal to zero, the beam-column changes to column. Inverse, in the beam-column, if the axial compression load is equal to zero, the beam-column changes to beam. The results showed that the CFRP sheet was more effective on the SHS steel beams than the SHS steel columns.
- Compared the specimen AC2-100 with the specimen BC2-100, when the lateral load increases in the beam-columns, it can be concluded that with an increase in section dimensions of the SHS steel beam-columns, the rate of increase of the ultimate load can be raised (see Tables 6 and 7).
- Compared the interaction curves of the Type A beam-columns with the Type B beam-columns, it can be observed that the shape of the interaction curves of the Type A beam-columns and the Type B are different. In all Type B beam-columns with a decrease in the axial compression load up to zero, the ultimate lateral load increases. Also, with a decrease in the axial compression load up to zero, the increase of the ultimate lateral load for all Type A beam-columns is not observed (see Fig. 6).

References

ACI Committee 440. (2002), "Guide for the design and construction of externally bonded FRP systems for strengthening concrete structures", *ACI440.2R-02*, Farmington Hills, MI, American Institute.

Abdollahi chakand, N. and Zamin Jumaat, M. (2013), "Experimental and theoretical investigation on torsional behavior CFRP strengthened square hollow steel section", *Thin Wall. Struct.*, **68**, 135-140.

Al Zand, A.W., Badaruzzaman, W.H. and Mutalib, A.A. (2015), "Qahtan AH. Finite element analysis of square CFST beam strengthened by CFRP composite material", *Thin Wall. Struct.*, **96**, 348-358.

Al-Zubaidy, H., Al-Mahaidi, R. and Zhao, X.L. (2013), "Finite element modelling of CFRP/steel double strap joints subjected to dynamic tensile loadings", *Compos. Struct.*, **99**, 48-61.

Bambach, M.R., Jama, H.H. and Elchalakani, M. (2009), "Axial capacity and design of thin-walled steel SHS strengthened with CFRP", *Thin Wall. Struct.*, **47**, 1112-1121.

Deng, J., Lee, M.M. and Moy, S.S. (2004), "Stress analysis of steel beams reinforced with a bonded CFRP plate", *Compos. Struct.*, **65**(2), 205-215.

Haedir, J. and Zhao, X.L. (2011), "Design of short CFRP-reinforced steel tubular columns", *J. Constr. Steel Res.*, **67**, 497-509.

Fanggi, B.A.L and Ozbakkaloglu, T. (2015), "Square FRP–HSC–steel composite columns: Behavior under axial compression", *Eng. Struct.*, **92**, 156-171.

Idris, Y. and Ozbakkaloglu, T. (2016). "Behavior of square fiber reinforced polymer–high-strength concrete–steel double-skin tubular columns under combined axial compression and reversed-cyclic lateral loading", *Eng. Struct.*, **118**, 307-319.

Idris, Y. and Ozbakkaloglu, T. (2014). "Flexural behavior of FRP-HSC-steel composite beams", *Thin Wall. Struct.*, **80**, 207-216.

Islam, S.Z. and Young, B. (2013), "Strengthening of ferritic stainless steel tubular structural members using FRP subjected to Two-Flange-Loading", *Thin Wall. Struct.*, **62**, 179-190.

Kim, Y.J. and Harries, K.A. (2011), "Behavior of tee-section bracing members retrofitted with CFRP strips subjected to axial compression", *Composites Part B: Eng*., **42**(4), 789-800.

Keykha, A.H., Nekooei, M. and Rahgozar, R. (2015), "Experimental and theoretical analysis of hollow steel columns strengthening by CFRP", *Civil Eng. Dimension*, **17**(2), 101-107.

Keykha, A.H., Nekooei, M. and Rahgozar, R. (2016b), "Numerical and experimental investigation of hollow steel columns strengthened with carbon fiber reinforced polymer", *J. Struct. Constr. Eng.*, **3** (1), 49-58.

Keykha, A.H., Nekooei, M. and Rahgozar, R. (2016a), "Analysis and strengthening of SHS Steel columns using CFRP composite materials", *Compos. Mech. Comput. Appl.*, **7**(4), 275-290.

Keykha A.H. (2017a), "Finite element investigation on the structural behavior of deficient steel beam-columns strengthened using CFRP composite", *Proceedings of the 3th international conference on mechanics of composites (MECHCOMP3)*, Bologna, Italy, July.

Keykha, A.H. (2017b), "CFRP strengthening of steel columns subjected to eccentric compression loading", *Steel Compos. Struct.*, **23**(1), 87-94.

Keykha A.H. (2017c), "Structural behaviors of deficient steel members strengthened using CFRP composite subjected to torsional loading, *Proceedings of the 3th international conference on mechanics of composites (MECHCOMP3)*, Bologna, Italy, July.

Keykha, A.H. (2017d), "Numerical investigation on the behavior of SHS steel frames strengthened using CFRP", *Steel Compos. Struct.*, **24** (5), 561-568.

Ozbakkaloglu, T. and Xie, T. (2015), "Behavior of steel fiber-reinforced high-strength concrete-filled FRP tube columns under axial compression", *Eng. Struct.*, **90**, 158-171.

Ozbakkaloglu, T. and Idris, Y. (2014), "Seismic behavior of FRP-high-strength concrete–steel double-skin tubular columns", *J. Struct. Eng.*, **140**(6), 04014019.

Idris, Y. and Ozbakkaloglu, T. (2015), "Flexural behavior of FRP-HSC-steel double skin tubular beams under reversed-cyclic loading", *Thin Wall. Struct.*, **87**, 89-101.

Park, J.W. and Yoo, J.H. (2013), "Axial loading tests and load capacity prediction of slender SHS stub columns strengthened with carbon fiber reinforced polymers", *Steel Compos. Struct.*, **15**(2), 131-150.

Sundarraja, M.C. and Prabhu, G.G. (2013), "Flexural behaviour of CFST members strengthened using CFRP composites", *Steel Compos. Struct.*, **15**(6), 623-643.

Teng, J.G. and Hu, Y.M. (2007), "Behavior of FRP jacketed circular steel tubes and cylindrical shells under compression", *Int. J. Constr. Build. Mater.*, **21**(4), 827-838.

Youssef, M.A. (2006), "Analytical prediction of the linear and nonlinear behaviour of steel beams rehabilitated using FRP sheets", *Eng. Struct.*, **28**(6), 903-911.